

## Supporting Information

### Crystal Structure of DNA Polymerase $\beta$ with DNA Containing the Base Lesion Spiroiminodihydantoin in Templating Position

Brian E. Eckenroth,<sup>1</sup> Aaron M. Fleming,<sup>2</sup> Joann B. Sweasy,<sup>3</sup> Cynthia J. Burrows,<sup>2</sup> and Sylvie Doublé<sup>1</sup>

<sup>1</sup>Department of Microbiology and Molecular Genetics, University of Vermont, Stafford Hall, 95 Carrigan Drive, Burlington, Vermont 05405, United States

<sup>2</sup>Department of Chemistry, University of Utah, 315 South 1400 East, Salt Lake City, Utah 84112, United States

<sup>3</sup>Department of Therapeutic Radiology, Yale University School of Medicine, New Haven, Connecticut 06520

## EXPERIMENTAL PROCEDURES

### Preparation of DNA Duplex

The 16-mer template strand containing (*S*)-dSp (5'-CCGAC-dSp1-GCGCATCAGC-3') was synthesized as previously described.<sup>1</sup> The strand purity was determined by HPLC (see below) and the product identity was determined by ESI-MS, in which the calculated mass = 4884.2 and experimental mass = 4884.0. The 10-mer primer strand (5'-GCTGATGCGC-3') and 5-mer downstream strand (5'-GTCGG-3') were synthesized by Midland Certified Reagent Company, Incorporated (Midland, TX). The three oligonucleotides were mixed in a 1:1:1.5 ratio in 20 mM Tris-HCl pH 7.5 with 20 mM MgCl<sub>2</sub> and heated to 95°C. The mixture was allowed to cool to room temperature then placed on ice for 10 min.

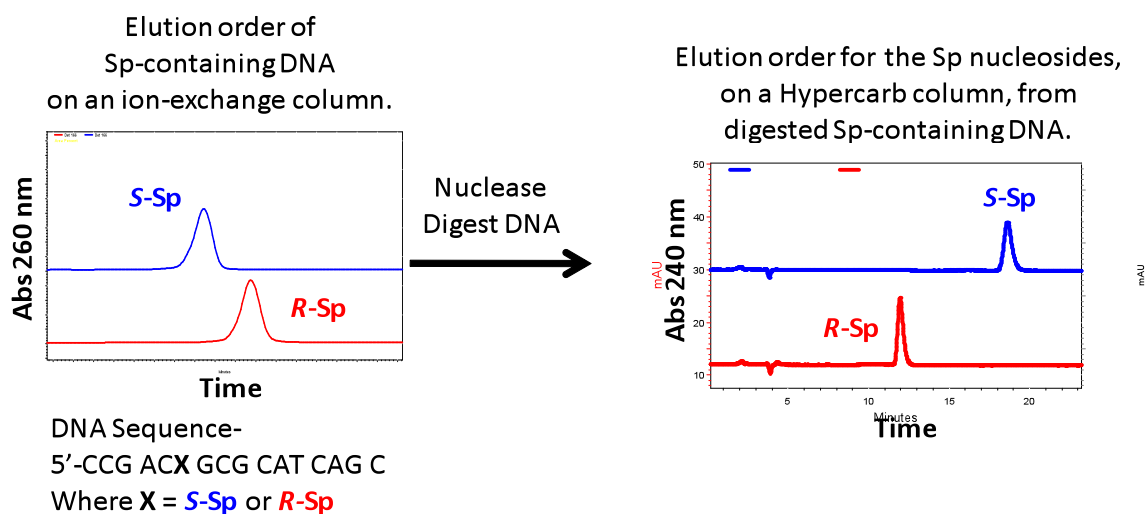
### Crystallization, data collection and refinement

Human DNA polymerase  $\beta$  variant E295K was purified as previously described and crystallized at 10 mg/ml in the presence of 2-fold molar excess of DNA duplex at 18°C.<sup>2</sup> The protein and DNA complex was mixed 1:1 with reservoir solution containing 50 mM Hepes pH 7.5, 150 mM sodium acetate and 12-16% (w/v) PEG 3350. Cryoprotection was achieved by soaking the crystals in reservoir solution containing 20% PEG 3350 and 14% (v/v) ethylene glycol. Crystals were flash cooled in liquid nitrogen and data were collected at 100K on a Rigaku RUH-3R rotating anode generator attached to Mar345 image plate. Data were processed with the HKL2000 suite<sup>3</sup> with model building in Coot v0.7<sup>4</sup> and refinement in Phenix v1.8.1.<sup>5</sup> The binary complex PDB ID 4M9G was used for isomorphous replacement with the lesion position along with two nucleotides in the 5' and 3' directions omitted from initial phase calculations for reduced bias electron density maps.<sup>2</sup> The Cross R on intensities between the two crystallographic data sets was 33%. Of the 335 residues for DNA polymerase  $\beta$ , 314 had sufficient electron density to be included in the final model with those omitted also disordered in previous binary structures. A Ramachandran plot indicated that 97.7% of residues are in the favored region, with no outliers. All figures were generated with PyMOL<sup>6</sup>. Comparison of additional structures was performed using least squares superposition of the catalytic domain of pol  $\beta$  (151-261).

**Table S1.** A comparison of DNA backbone torsion angles generated using the 3DNA server<sup>7-9</sup> for DNA pol  $\beta$  E295K bound to DNA containing dA (Complex 1)<sup>2</sup> or (*S*)-dSp (Complex 2) in templating position vs. WT DNA pol  $\beta$  with dG (Complex 3)<sup>10</sup> or 8-oxoG *syn*<sup>11</sup> (Complex 4). Highlighted are the most significant deviations using Complex 3 as reference.

Complex 1 E295K pol $\beta$ dA templating (PDB ID 4M9G)							
Base	$\alpha$	$\beta$	$\gamma$	$\delta$	$\epsilon$	$\zeta$	pucker
5'-C	-70.2	160.4	51.5	91.4	-159.3	64.5	O4'-endo
dA	63.5	155.8	55.6	142.5	178.1	-96.5	C3'-exo
3'-G	-56.2	169.3	56.3	126.3	-172.1	-108.3	C1'-exo
Complex 2 E295K pol $\beta$ ( <i>S</i> )-dSp templating (4PPX)							
Base	$\alpha$	$\beta$	$\gamma$	$\delta$	$\epsilon$	$\zeta$	pucker
5'-C	-60.4	169.1	44.4	124.3	-79.3	-70.9	C1'-exo
dSp1	-64.7	177.9	-90.1	160.1	-126.7	-163.8	C2'-endo
3'-G	-53.8	147.9	39.8	139.3	-179.9	-114.0	C2'-endo
Complex 3 WT pol $\beta$ dG templating (PDB ID 3ISB)							
Base	$\alpha$	$\beta$	$\gamma$	$\delta$	$\epsilon$	$\zeta$	pucker
5'-C	-56.1	165.0	39.5	104.6	-168.1	59.7	O4'-endo
dG	66.5	153.4	49.6	149.9	-162.0	-147.9	C2'-endo
3'-G	-30.8	135.5	49.8	138.8	-161.6	-127.7	C2'-endo
Complex 4 WT pol $\beta$ 8-oxoG templating (PDB ID 3RJE)							
Base	$\alpha$	$\beta$	$\gamma$	$\delta$	$\epsilon$	$\zeta$	pucker
5'-C	-56.4	166.9	34.1	115.0	-65.6	-83.2	C1'-exo
8-oxoG <i>syn</i>	159.6	172.1	60.9	114.0	-167.4	-111.1	C1'-exo
3'-T	-44.6	140.2	68.7	99.7	-168.5	-95.4	O4'-endo

**Figure S1.** Chromatograms demonstrating the purity of the Sp oligonucleotide, and the elution order switching between ion-exchange and Hypercarb HPLC columns.



In previous studies it was demonstrated that the elution order of Sp switches based on the HPLC column used for the analysis. When Sp is in an oligodeoxynucleotide context and analyzed by ion-exchange HPLC, (*S*)-Sp elutes first, whereas when the Sp nucleosides are analyzed by Hypercarb HPLC (*R*)-Sp elutes first. To ensure that (*S*)-Sp (Sp1) in the current study is the same as all reports concerning Sp stereochemistry, the Sp-containing oligodeoxynucleotide was digested to nucleosides and analyzed by Hypercarb HPLC, and as expected the elution order switched between the columns. See reference 1 for further details.

Ion-exchange HPLC conditions: Dionex DNAPac PA100 running A = 1:9 (v/v) MeCN:ddH<sub>2</sub>O, and B = 1.5 M NaOAc (pH 7) in 1:9 (v/v) MeCN:ddH<sub>2</sub>O with a flow rate = 1 mL/min while monitoring the absorbance at 260 nm. The method was initiated at 15% B followed by a linear increase to 100% B over 30 min.

Hypercarb HPLC conditions: Thermo 150 x 4.6 mm running A = 0.1% acetic acid and B = MeOH with a flow rate = 1 mL/min while monitoring the absorbance at 240 nm. The method was initiated at 0% B and held for 20 min followed by a linear increase to 75% B over 20 min.

**Figure S2.** Comparison of WT pol  $\beta$  with dG in templating position (PDB ID 3ISB)<sup>10</sup> shown in black to that of the E295K variant with dA (PDB ID 4M9G)<sup>2</sup> shown in grey or (*S*)-dSp (cyan). The  $F_o - F_o$  isomorphous difference Fourier map<sup>12,13</sup> shown is between the E295K dA and (*S*)-dSp and contoured at  $+3\sigma$  (green mesh) and  $-3\sigma$  (red mesh). The A-ring of (*S*)-dSp is indicated.

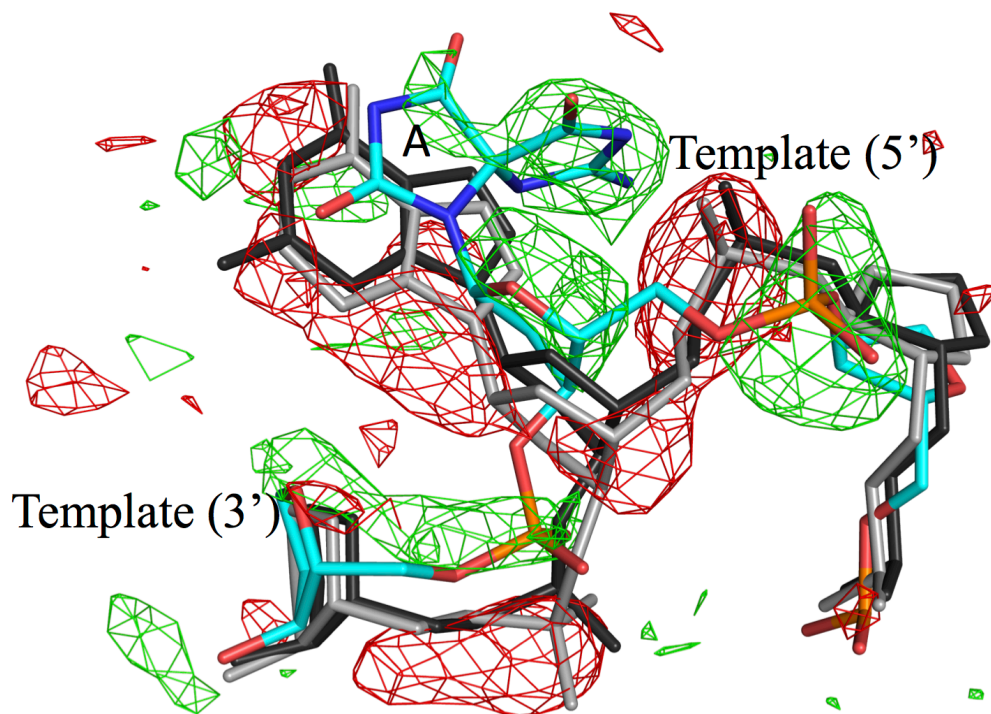
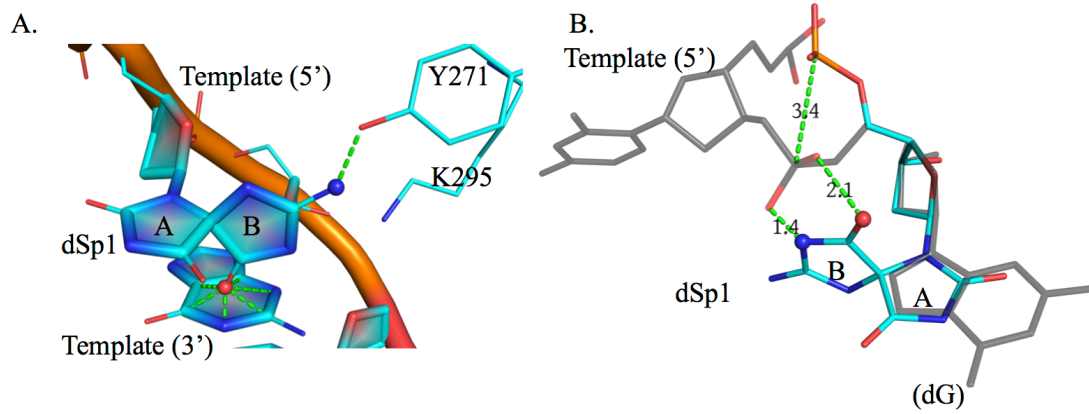


**Figure S3.** Demonstration of atomic clashes likely to lead to adoption of the *syn* conformation of (*S*)-dSp in the DNA duplex bound to pol  $\beta$ . All clash distances range from 1.1 to 2.1 Å. **A.** Shown is the rotation of the (*S*)-dSp into the *anti* conformation. **B.** The DNA duplex containing (*S*)-dSp shown in cyan superimposed with DNA duplex containing dG shown in black (PDB ID 3ISB)<sup>10</sup> without the necessary backbone rearrangement to accommodate the B-ring of the lesion.



## REFERENCES

- (1) Fleming, A. M., Orendt, A. M., He, Y., Zhu, J., Dukor, R. K., and Burrows, C. J. (2013) Reconciliation of chemical, enzymatic, spectroscopic and computational data to assign the absolute configuration of the DNA base lesion spiroiminodihydantoin. *J. Am. Chem. Soc.* *135*, 18191-18204.
- (2) Eckenroth, B. E., Towle-Weicksel, J. B., Sweasy, J. B., and Doubl  , S. (2013) The E295K cancer variant of human polymerase beta favors the mismatch conformational pathway during nucleotide selection. *J. Biol. Chem.* *288*, 34850-34860.
- (3) Otwinowski, Z., and Minor, W. (1997) Processing of X-ray diffraction data collected in oscillation mode. *Method Enzymol* *276*, 307-326.
- (4) Emsley, P., and Cowtan, K. (2004) Coot: model-building tools for molecular graphics. *Acta Crystallogr D* *60*, 2126-2132.
- (5) Adams, P. D., Afonine, P. V., Bunkoczi, G., Chen, V. B., Davis, I. W., Echols, N., Headd, J. J., Hung, L. W., Kapral, G. J., Grosse-Kunstleve, R. W., McCoy, A. J., Moriarty, N. W., Oeffner, R., Read, R. J., Richardson, D. C., Richardson, J. S., Terwilliger, T. C., and Zwart, P. H. (2010) PHENIX: a comprehensive Python-based system for macromolecular structure solution. *Acta Crystallogr. D Biol. Crystallogr.* *66*, 213-221.
- (6) The PyMOL Molecular Graphics System. *Schrodinger, LLC Version 1.5.0.5*.
- (7) Lu, X. J., and Olson, W. K. (2008) 3DNA: a versatile, integrated software system for the analysis, rebuilding and visualization of three-dimensional nucleic-acid structures. *Nat. Protoc.* *3*, 1213-1227.
- (8) Zheng, G., Lu, X. J., and Olson, W. K. (2009) Web 3DNA--a web server for the analysis, reconstruction, and visualization of three-dimensional nucleic-acid structures. *Nucleic Acids Res.* *37*, W240-246.
- (9) Zheng, G., Colasanti, A. V., Lu, X. J., and Olson, W. K. (2010) 3DNALandscapes: a database for exploring the conformational features of DNA. *Nucleic Acids Res.* *38*, D267-274.
- (10) Beard, W. A., Shock, D. D., Batra, V. K., Pedersen, L. C., and Wilson, S. H. (2009) DNA polymerase beta substrate specificity: side chain modulation of the "A-rule". *J. Biol. Chem.* *284*, 31680-31689.
- (11) Batra, V. K., Shock, D. D., Beard, W. A., McKenna, C. E., and Wilson, S. H. (2012) Binary complex crystal structure of DNA polymerase beta reveals multiple conformations of the templating 8-oxoguanine lesion. *Proc. Natl. Acad. Sci. U. S. A.* *109*, 113-118.
- (12) Rould, M. A., and Carter, C. W., Jr. (2003) Isomorphous difference methods. *Methods Enzymol.* *374*, 145-163.
- (13) Rould, M. A. (2007) The same but different: isomorphous methods for phasing and high-throughput ligand screening. *Methods Mol. Biol.* *364*, 159-182.